Interface superconductivity

Gariglio, Stefano; Gabay, M.; Mannhart, J.; Triscone, Jean-Marc

How to cite

GARIGLIO, Stefano et al. Interface superconductivity. In: Physica. C, Superconductivity, 2015, vol. 514, p. 189–198. doi: 10.1016/j.physc.2015.02.028

This publication URL: https://archive-ouverte.unige.ch//unige:72785
Publication DOI: 10.1016/j.physc.2015.02.028

Interface Superconductivity

S. Gariglio[a,*], M. Gabay[b], J. Mannhart[c], J.-M. Triscone[a]

[a] *DQMP, Université de Genève, 24 Quai E.-Ansermet CH-1211 Genève, Switzerland*
[b] *Laboratoire de Physique des Solides, Bat 510, Université Paris-Sud 11, Centre d'Orsay, 91405 Orsay Cedex, France*
[c] *Max Planck Institute for Solid State Research, 70569 Stuttgart, Germany*

Abstract

Low dimensional superconducting systems have been the subject of numerous studies for many years. In this article, we focus our attention on interfacial superconductivity, a field that has been boosted by the discovery of superconductivity at the interface between the two band insulators $LaAlO_3$ and $SrTiO_3$. We explore the properties of this amazing system that allows the electric field control and on/off switching of superconductivity. We discuss the similarities and differences between bulk doped $SrTiO_3$ and the interface system and the possible role of the interfacially induced Rashba type spin-orbit. We also, more briefly, discuss interface superconductivity in cuprates, in electrical double layer transistor field effect experiments, and the recent observation of a high T_c in a monolayer of FeSe deposited on $SrTiO_3$.

1. Introduction

Low dimensional systems have had an enduring fascination for the condensed matter community. This is understandable from the perspective of fundamental research since disorder, fluctuations and correlation effects all play a particularly important role in reduced dimensions and thus offer opportunities to tackle tough theoretical and experimental challenges. It may seem more surprising insofar as applied research is concerned. While engineering bulk material compo-

*Corresponding author
Email address: stefano.gariglio@unige.ch (S. Gariglio)

nents, such as memristors, is being actively pursued, the ubiquity of nanowires and two-dimensional (2D) electron gases in our current technology is evidence for the merit of transport in confined geometries. Several considerations help explain this apparent paradox. One is that the increasing versatility of functionalities in portable electronic devices requires one to pack and connect more and more transistors on centimeter square size chips. Two, charge control through electric fields – i.e. gating – is more effective in lower dimensions as screening effects become more relevant. Furthermore, fluctuations effects, correlations effects and nesting of potentially significant portions of the Fermi surface in lower dimensions are factors that promote the appearance of novel quantum electronic states, paving the way for promising future technologies; in this respect, copper oxide superconductors could qualify as a Rosetta stone, owing to their quasi-2D, layered, structure, to the large value of the on-site electron-electron Coulomb repulsion, and to the strong antiferromagnetic correlations that are observed in a broad region of their phase diagram. The latter are advocated in some models to be the source of the pairing energy for superconductivity and the reason for the observed high value of the transition temperature T_c.

Historically, nesting of the Fermi surface was envisioned as an effective way to boost T_c [1]. It causes Van Hove singularities, implying high densities of states when the Fermi energy is tuned to a singularity. There were hopes that this scenario would help one attain high temperature superconductivity (HTSC), despite the fact that, in accordance to the Peierls-Mermin-Wagner theorem, thermal fluctuations preclude the establishment of long range order in one-dimensional (1D) and in 2D systems. For 1D organic materials nesting effects are particularly pronounced but fluctuations, unfortunately, promote competing instabilities of the Fermi sea and the attained values of T_c remain fairly small [2]. Thermal fluctuations in layered materials such as cuprates or in superconducting films have a "milder" impact on T_c.

More recently, the discovery of interfacial superconductivity in heterostructures whose building blocks consist of transition metal oxide compounds has attracted a lot of attention. A frontrunner in that category is the interface

between the two band-insulators $LaAlO_3$ (LAO) and $SrTiO_3$. It was found to be conducting (in 2004 [3]), superconducting (in 2007 [4]), and host to a sizable spin-orbit interaction (in 2010 [5, 6]). Quite remarkably, all these properties, conductivity, superconductivity and spin-orbit strength can be controlled by an electric field. In copper-oxide based heterostructures, where none of the constituents exhibit superconductivity, HTSC was demonstrated to develop in a single atomic CuO_2 plane [7]. Evidence for high T_c superconductivity has also been reported for FeSe atomically thin films prepared on $SrTiO_3$ [8]. Using the electrical double layer transistor (EDLT) technique, which allows one to achieve very large changes in carrier density, it is possible to induce superconductivity at the surface of insulating crystals [9] and to dramatically tune the value of the superconducting T_c at the surface of known superconductors [10].

The possibility of boosting T_c at metallic surfaces embedded in otherwise semiconducting or even insulating materials has been advocated by several authors. The driving force for the increase is a spatial dichotomy between Cooper pairs which reside in the conducting sheet, and the source of pairing which originates from the "non-metallic" bulk part. Accordingly, the adverse impact of the Coulomb repulsion on superconductivity is somewhat lessened [11]. Near the interface, on the pairing side, the density of states can be much enhanced [12, 13]. Besides, large attractive interactions between electrons of the surface sheet can be mediated by excitations coming from the unscreened (or poorly screened) bulk region; for instance, these can be excitonic [14] or driven by polarization effects [15, 16, 17]. This is shown in Fig. 1. A similar scenario has been proposed in the context of LAO/STO compounds in order to model the evolution of T_c with doping [18].

In this paper, we will focus our attention on the prototypical LAO/STO interface, discussing the physics of this system, the relation between interfacial and bulk superconductivity observed in doped STO, the nature of superconductivity and the role possibly played by spin-orbit interaction. We will also, briefly, discuss other systems of interest that have been studied recently.

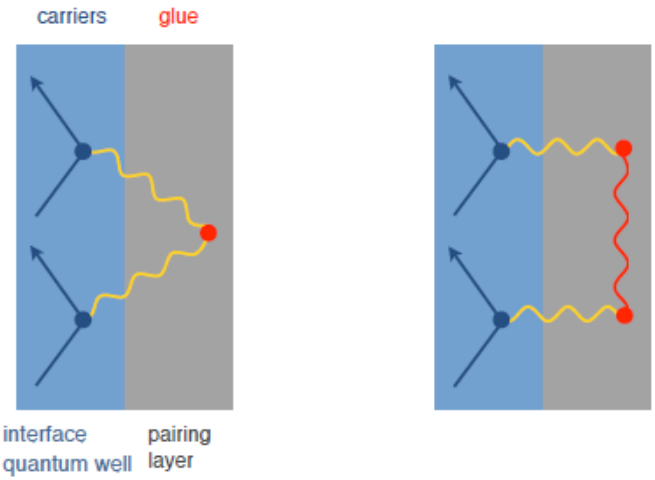

Figure 1: (Left) Two electrons (blue) interact (yellow) with a site (red) in the pairing layer, creating a virtual excitation. This excitation, for example polarization of an oxygen ion, causes the pairing. (Right) Each electron excites a different site in the pairing layer, but both sites are coupled (red), and by this close the pairing channel.

2. Some history and progress in oxide thin film technology

In the 80's, there have been many important studies of metallic low-dimensional superconducting systems (ultrathin films, and superlattices). Those include experiments on Kosterlitz-Thouless physics, the role of disorder, superconductor-insulator transitions, dimensional crossovers, and related effects. There is unfortunately too little space here to describe these remarkable contributions. Some of the achievements and references can be found in the article "Superconductivity of Very Thin Films: The Superconductor-Insulator Transition" by Lin, Nelson and Goldman in this special issue and in the book "Synthetic Modulated Structure" [19].

Following the discovery of high T_c superconductors, a large effort has been devoted to growing epitaxial films of complex oxides. 28 years later, these developments allow oxide heterostructures with atomically sharp interfaces to be grown using several techniques including molecular beam epitaxy, pulsed laser deposition and sputtering. A more recent advance in the area of oxide het-

erostructures concerns oxide interfaces. Thanks to the chemical and structural compatibility of many oxides, these structures have allowed materials with very different electronic properties to be combined. The further use of strain, confinement or more generally interfacial effects has given rise to a variety of exciting work; we refer here to the reviews of J. Mannhart, and D. G. Schlom [20], P. Zubko *et al.* [21] and H. Y. Hwang *et al.* [22]. This new research area has been developing rapidly after the seminal work of Akira Othomo and Harold Hwang who studied $LaTiO_3/SrTiO_3$ - an interface between a Mott and a band insulator [23] - and $LaAlO_3/SrTiO_3$, an interface between two band insulators[3]. The discovery of conductivity and high electron mobility at the interface between LAO and STO generated a large amount of work aiming at an understanding of the origin of the conduction and at the exploration of the properties of these mobile electrons hosted in a complex oxide. As we will see, this system indeed displays amazing properties.

3. The LAO/STO system

In their bulk state, both LAO and STO are insulators with a sizable band gap of 5.6 eV and 3.2 eV - respectively. It was found that the growth on an epitaxial film of LAO on a (001)-oriented TiO_2-terminated single crystal of STO leads to a conducting interface if the LAO thickness is larger than three unit cells [24]. Early on, the origin of the metallic state has been linked to the existence of a polar discontinuity across the LAO/STO interface [25]. While both SrO and TiO_2 layers are charge neutral on the STO side of the (001) oriented structure, LaO and AlO_2 sheets, by contrast, carry positive and negative charge, respectively, in the LAO film. The ensuing charge discontinuity at the interface leads to a potential difference between the interface and the LAO surface. This potential difference grows with increasing LAO thickness. Several scenarios have then been proposed in order to explain how the polar field is compensated within the LAO film, beyond three unit cells. For instance a Zener breakdown could occur, causing charge transfer from the LAO surface to the interface, thereby screening the field [26, 27, 28]. Alternatively, oxygen vacancies located at the

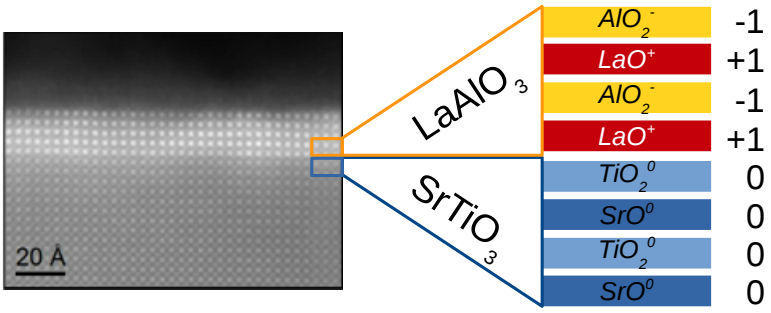

Figure 2: The LAO/STO interface structure. TEM image of the interface (from Ref. [4]) and schematics of the alternating atomic planes along the [001] direction: SrO and TiO_2 planes in $SrTiO_3$ are neutral, whereas the LaO and AlO_2 planes are charged +1 and -1, respectively.

LAO surface have been advocated as the providers of electrons required to heal the discontinuity [29, 30]. Oxygen vacancies on the STO side of the interface and / or cation intermixing across the interface [31, 32] have also been invoked as a possible source for the conduction observed - note that those do not imply a charge transfer from the LAO surface to the LAO/STO interface and thus do not solve the polar catastrophe problem [33].

To fully cancel the polar field, the transferred surface charge density should be 0.5 e/planar unit cell or 3 10^{14} e cm^{-2}. The transferred electrons are located on the STO side, close to the interface; they populate the Ti 3d band (initially Ti is in the Ti^{4+} state) filling the t_{2g} orbitals and they change the Ti valence from 4+ to 3+ for a fraction of the sites. Figure 2 shows the atomic structure of the interface as seen by TEM [4] and the stacking of the atomic layers with the polar discontinuity at the interface.

As mentioned above, electrons are in the Ti 3d bands and are confined at the interface. Several experiments have been probing the extension of the conducting layer. Using conducting AFM in a cross-section geometry [34], optical spectroscopy [35] or the anisotropy of the superconducting properties [36], it is found that the conducting layer has a characteristic width at low temperatures of about 10 nm. This confinement and breaking of inversion symmetry has two important consequences. One is to lift the t_{2g} orbital degeneracy and to produce a sub-band structure; two is to induce a Rashba type spin-orbit. We will come

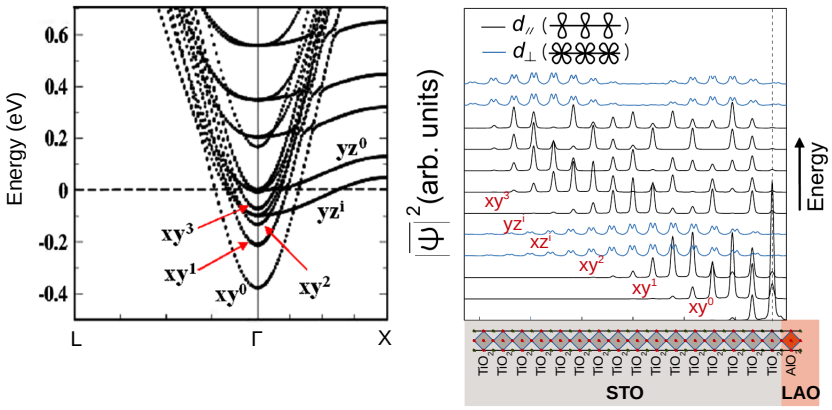

Figure 3: (Left) Electronic sub-band structure in the Brillouin zone calculated for the LAO/STO interface by Delugas *et al.*[37]. (Right) Spatial dependence of the square of the associated sub-band eigenfunctions in the direction perpendicular to the interface; $d_{||}$ refers to d_{xy} orbitals while $d_{\perp}$ refers to d_{xz}/d_{yz} orbitals (from Ref. [38]). The orbital character of the states is shown in both panels; for each orbital a superscript labels the energy of the band at the Gamma point. One notices that, for the first three d_{xy} sub-bands, it also identifies the location of the TiO_2 layer counted from the interface where the probability of presence of the carriers in that band is dominant.

back to this second point later.

Salluzzo and co-workers were the first authors to experimentally show that the degeneracy of the t_{2g} orbitals is indeed lifted [39]. Confinement is pushing the heavy d_{xz} and d_{yz} orbitals to higher energies. Electronic states pertaining to the lowest energy sub-bands describe carriers essentially localized in the vicinity of the interface and the first three sub-bands have d_{xy} character (Figure 3). The right panel in Figure 3 shows the spatial dependence of the square of low energy sub-band eigenfunctions in the direction perpendicular to the interface; the array is generated by setting the energy equal to the increasing order sequence of eigenenergies. Note that these functions exhibit narrow peaks centered on consecutive TiO_2 layers, consistently with the dominant d character of the conduction bands. The orbital character of each band is indicated on both panels of Figure 3, along with a superscript which identifies the energy of the band at the Gamma point. The physics of the confined d shell states is far richer and more complex than that encountered in the case of p-orbital states of electron gases in semiconductors. Tunneling experiments in the normal state

indeed reveal a complex conductance versus energy pattern that could only be fitted using a LDA+U approach suggesting that correlations are at play at the LAO/STO interface [40]. Thus, instead of using the terminology 2D electron gas one should refer to this as 2D electron liquid (2DEL).

Comparing Fig. 3 with the calculations of the electronic structure of bulk STO[41], one notices that the confinement of the 2DEL is leading to an "inversion" of the band structure with the lowest (sub-)bands at the interface having an xy character - in the bulk, the lowest band is an hybridized band with heavy character for moderate fillings. The interfacial electronic structure is thus very different from that in the bulk. This is of importance and we will come back to this point when discussing superconductivity.

The confinement of the electron liquid and breaking of inversion symmetry also lead to a Rashba type spin-orbit whose strength is related to the carrier density. In this system, the carrier density can be tuned using an electric field. Indeed, since the conducting layer is in-between two insulators, the field effect can be used with a top, side or back gate geometry, and allows the carrier density to be continuously controlled. As we will see below, changing the doping also allows a control of superconductivity. Regarding spin-orbit, magnetoresistance measurements were performed with the field applied perpendicular to the conducting plane [5]. As the carrier density was increased, the magnetoresistance curves showed a crossover from a weak localization regime at low doping to a weak anti-localization regime at higher doping. Data analysis allowed the spin-orbit strength to be extracted along with the relation between the spin-orbit scattering time (τ_{so}) and the elastic scattering time (τ_e) revealing that τ_{so} goes as τ_e^{-1}. This dependence points to the Dyakonov-Perel mechanism, as one might expect when a spin-orbit interaction of the Rashba type is at play. This spin-orbit is thus a signature of the breaking of inversion symmetry at the interface. The maximum spin-orbit strength is on the order of 10 meV, which is much larger than the superconducting gap (of the order of 40 μeV [42]).

Beyond the spin-orbit interaction, several signatures of magnetism have been reported in the LAO/STO system. The Twente group first reported that, for

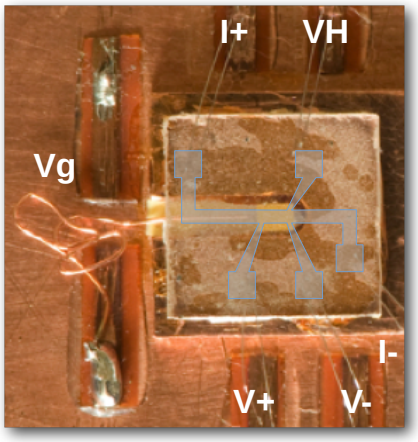

Figure 4: A photograph of the field effect device with a drawing of the Hall bar. The size of the STO crystal is 5 mm by 5 mm and the conducting channel is 500 μm wide.

samples grown at high oxygen pressures, resistance versus temperature curves showed a dependence reminiscent of a Kondo system [43]. The simultaneous occurrence of magnetism and superconductivity was found in torque measurements, which indicated some type of magnetic ordering [44], but also in scanning SQUID experiments which detected a patchwork of magnetic domains [45] and in magnetoresistance measurements [46]. The link between these different experimental results is at the moment not very clear. Models on the origin of the magnetism and on the possible relation between magnetism and superconductivity will be discussed below.

3.1. Superconductivity

Fig. 4 shows the field effect device configuration that has been used in most of the experiments. The STO substrate is used as a gate dielectric, the back gate voltage is controlling the doping of the system. Fig. 5 shows that a change in the doping causes a continuous tuning of the superconducting transition and the observation of a superconductor to insulator transition. A reversible on/off electric field switching of superconductivity at low temperatures is thus possible in this system.

We notice the dome-shaped aspect of the boundary between the supercon-

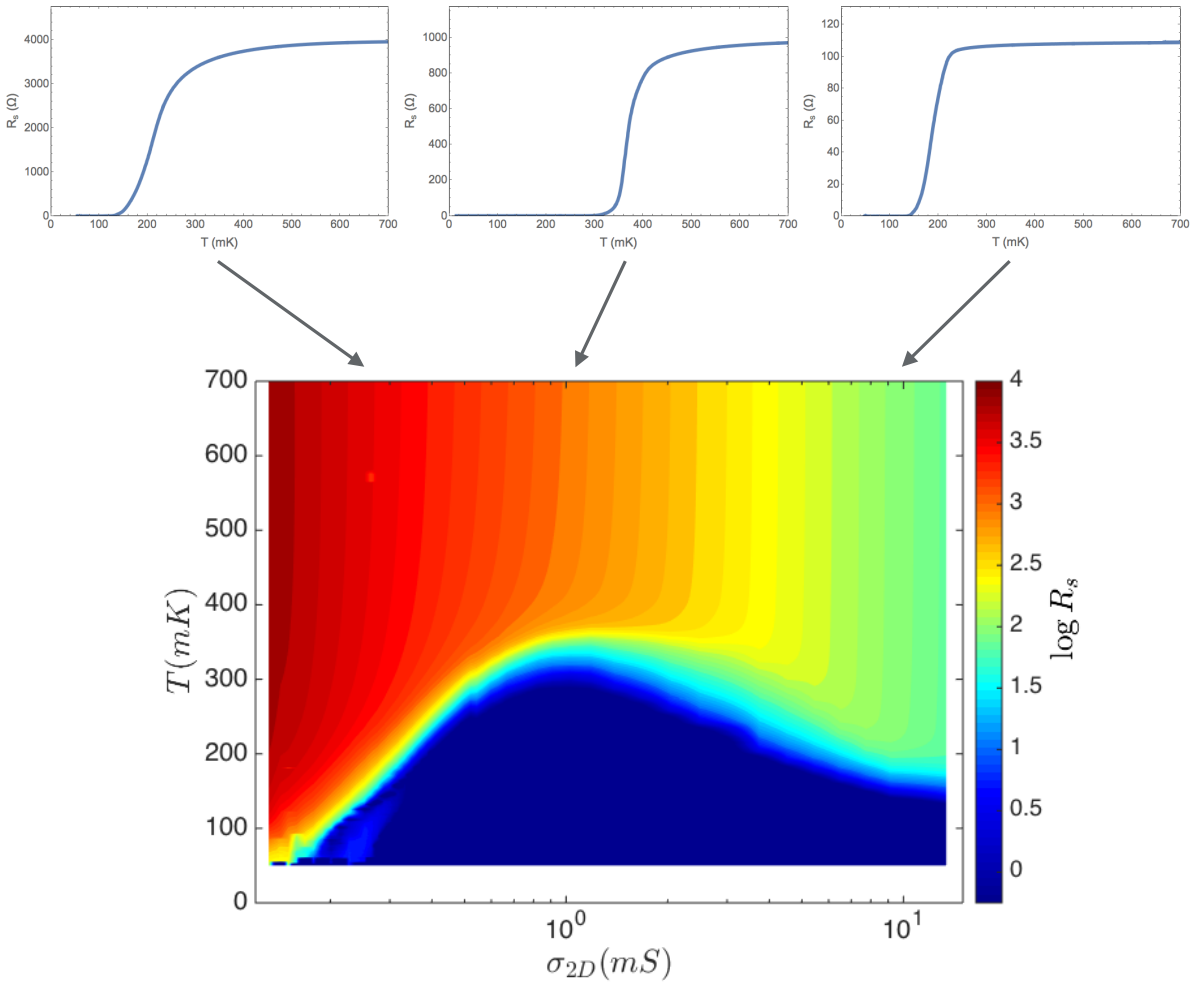

Figure 5: Phase diagram revealing the superconducting dome. (Top) Sheet resistance as a function of temperature for three different dopings - notice the different sheet resistance scales. (Bottom) Evolution of the sheet resistance (in log scale) in temperature for different dopings, represented by the conductance at 700 mK.

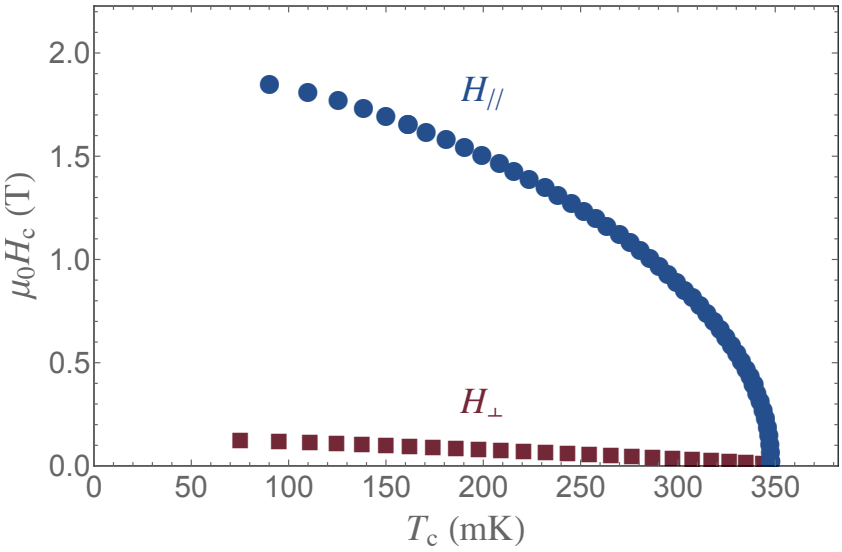

Figure 6: $H_{c\parallel}$ and $H_{c\perp}$ as a function of temperature for an optimally doped sample.

ducting and normal regions with an "underdoped" and an "overdoped" regime. The maximum T_c is around 300 mK. As one crosses the phase diagram, the sheet resistance changes dramatically, in fact much faster than the carrier density, pointing to a mobility that increases way more than the doping does. As mentioned above, the spin-orbit strength is also increasing rapidly as one is moving across the phase diagram [5].

Critical field measurements performed in the perpendicular and parallel geometries reveal a large anisotropy and a behavior characteristic of 2D superconductors [36]. Fig. 6 shows $H_{c\parallel}$ and $H_{c\perp}$ as a function of temperature for an optimally doped sample. From $H_{c\perp}$, one obtains the superconducting coherence length $\xi(T) = \sqrt{\phi_0/2\pi\mu_0 H_{c\perp}(T)}$ which is found to be about 60 nm at $T = 0$ K. From the analysis of $H_{c\parallel}$, one extracts the superconducting thickness d: $d = \sqrt{3}\phi_0/\pi\xi\mu_0 H_{c\parallel}$, here about 10 nm. Since this value is much smaller than the coherence length, the system is a 2D superconductor. $H_{c\parallel}$ and $H_{c\perp}$ measurements across the phase diagram reveal that the system is always in the 2D regime: the superconducting thickness is however found to increase as one is moving to the "overdoped" regime. The coherence length follows a roughly $1/T_c$

dependence. The largest values of the critical parallel fields, attained around optimal doping, are found to be about three times larger than the paramagnetic limit (that is $1.83\,T_c$ (T)). This increase is most probably linked to the spin-orbit as discussed below.

Since the system is 2D, one naturally expects fluctuations to play an important role and a Kosterlitz-Thouless (KT) transition to possibly control the establishment of phase coherence. $I-V$ characteristics were suggestive of such a transition but no clear jump in the a exponent ($V = I^a$) could be observed, raising questions about the occurrence of such transition. Also, the behavior of T_c versus gate voltage, T_c going as $(V_g - V_{gc})^{2/3}$ was taken as some evidence for an XY (fluctuations) scenario. More recently, tunneling experiments performed in Stuttgart revealed a pseudogap behavior in the underdoped regime [42]. The phase diagram observed looks very much like that of HTSC though rescaled. This "pseudogap" behavior could be a signature of a region of the phase diagram with paired electrons or superconducting fluctuations but without phase coherence, a scenario in-line with a KT transition. Another interpretation of these data is proposed by Benfatto and Giamarchi [47], and by Grilli and coworkers [48, 49, 50] who suggest that inhomogeneities may allow some of the observed behaviors to be understood (see also Ref. [51]). In these models, small inhomogeneities in the T_c or density inhomogeneities may lead to percolative transitions. More experiments will be necessary to determine the exact nature of the transitions and, in case of a "phase separation" scenario, to experimentally establish the presence of inhomogeneities and to understand their origin.

3.2. Bulk and interface superconductivity

Bulk STO has been known to host superconductivity since the sixties [52]. STO can be doped either through atomic substitutions (La for Sr, Nb for Ti), or through a reduction of the oxygen content. As a function of the carrier density, T_c displays a dome-like structure with a maximum critical temperature of about 300 mK [53, 54]. While the maximum T_c is about the same for both LAO/STO and bulk STO, the doping range over which superconductivity is

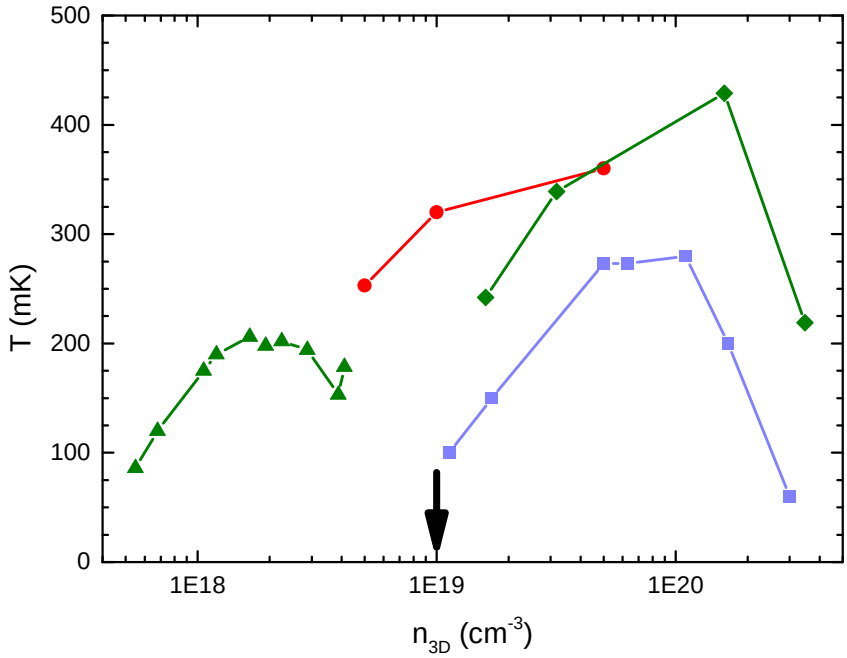

Figure 7: T_c versus doping for bulk doped $SrTiO_3$. Filled blue square symbols (■) show T_c zero for oxygen-reduced and Nb-doped crystals from Ref. [54]; filled green triangles (▲) and filled green diamonds (♦) correspond to the estimated value of T_c at 50% of the resistive transition for oxygen reduced crystals and for Nb-doped crystals respectively, from Ref. [55]; red circles (●) represent T_c estimated at 50% of the resistive transition for Nb-doped $SrTiO_3$ single crystals measured in Geneva. The arrow indicates the position of the beginning of the superconducting dome for LAO/STO interfaces. Lines are a guide to the eye.

found in crystals is broad. Figure 7 shows the bulk T_c versus the 3D carrier density reported in various studies [54, 55] along with our own data on Nb-doped STO crystals. Also shown is the 3D carrier density at which superconductivity develops for the LAO/STO interface. To translate a 2D sheet carrier density into a 3D, we chose a thickness of 10 nm which is the value that is derived from the $H_{c\parallel}$ - $H_{c\perp}$ analyses in the underdoped regime.

As can be seen, the bulk T_c develops at very low doping and superconductivity extends over a very wide range. The shape of the T_c versus doping curves obtained by Lin et al. are possibly linked to the filling of different bands [55]. Interfacial superconductivity develops only around a density of about $1\,10^{19}\,\mathrm{cm}^{-3}$. The observed behaviors are thus quite different and one should now identify the

differences between the two systems and pinpoint those which affect superconductivity.

Comparing the two systems, one notices that the level of disorder is different, the LAO/STO interface being clearly more disordered as the value $k_F l$ is about one around $5\,10^{18}\,\mathrm{cm}^{-3}$. Also, in the interfacial system, 2D fluctuations might play a role. However, the most important difference is linked to the electronic structure. In the bulk, the lowest band is a "heavy" band. At the interface, because of the electron confinement, the lowest sub-bands have a light d_{xy} character (Fig.2). Heavy bands have a high density of states that is very favorable for superconductivity. In the LAO/STO system, magnetotransport analyses suggest that the heavier xz, yz sub-bands start to be filled close to the doping level at which superconductivity develops [56]. One tempting scenario, supported by recent calculations, is that the main difference between the two systems is the band structure and the band "inversion" occurring at the interface. If correct, this would highlight key differences between bulk and interfacial superconductivity. The onset of superconductivity would also be a way to detect the filling of these subbands.

One further interesting question is linked to the superfluid density at the LAO/STO interface. Scanning SQUID experiments yield a very low value of the superfluid density in this system [57, 58]. Although no comparison has been made with bulk doped STO, a tempting explanation for these low values is that only d_{xz}/d_{yz} heavy electrons (that appear at the underdoped end-point of the dome) pair thus naturally explaining that the superfluid density is low, most of the interfacial carriers being xy in character and not participating to the superfluid density.

In the previous sections we highlighted several genuinely unconventional features that are hallmarks of electronic states and charge transport in the 2DEL formed at the $LaAlO_3/SrTiO_3$ interface and that are not usually encountered in III-V semiconductors. But there is more to it, as will become clear when we discuss spin related effects.

The spin and momentum of the charge carriers in the 2DEL are entangled,

due to the so called interfacial (Rashba) spin-orbit interaction, a signature of the breaking of inversion symmetry at the $LaAlO_3/SrTiO_3$ interface [5, 6]. The size of the Rashba energy rises by one order of magnitude upon gate-tuning a small increase of the charge concentration. This steep variation appears to correlate with the point when d_{xz} and d_{yz} states start contributing to transport at the Fermi level; around the voltage giving the highest superconducting T_c (optimal doping), the characteristic Rashba energy that is measured corresponds to a value on the order of 10 meV, comparable to the kinetic energy of the d_{xz} and d_{yz} carriers[56]. This impacts the normal phase, as it entails a reconstruction of the Fermi surface, possibly causing the appearance of a regime of protected transport (evidenced by a surge in the mobility) but this also affects the superconducting state, in two respects. The symmetry of the order parameter is not as simple as in a standard s-wave BCS case, in particular since there are intra- but also inter- Rashba bands pairings. In addition, applying an in-plane magnetic field may lead to helical FFLO ground states [59, 60, 61, 62] giving rise to a significant enhancement of the value of the critical field $H_{c2//}$, far beyond the Pauli limit.

Further manifestations of spin effects in LAO/STO heterostructures come from several independent experimental reports of ferromagnetism [44, 45, 46, 63, 64]. This came as a big surprise, considering that, in their bulk state, neither LAO nor STO show any sign of magnetism. While magnetic patches were detected using scanning SQUID microscopy with a very small average moment per interface unit cell area of 0.02 Bohr magneton, torque measurements revealed a large response with an average moment per interface unit cell area of 0.3 Bohr magneton. Furthermore, experiments performed at Stanford [65] did not seem to reveal any particular sensitivity of the magnetic response to the external electric field. These results raise a number of issues that are currently under intense scrutiny. Is magnetism intrinsic or extrinsic? In other words is it a property constitutive of the electronic states of the 2DEL or is it caused by defects, such as oxygen vacancies? In the former case, one needs to explain how magnetism may coexist with superconductivity, given that estimates of its characteristic energy

scale lead to values one order of magnitude larger than the Rashba spin-splitting and four order of magnitudes larger than the superconducting gap [60, 66]. In the latter case, the concentration of defects that is required to account for the number of moments would be extremely large [67]. At this stage it is not even agreed that all samples consistently exhibits magnetic signatures [68, 69] and, for those who do, one needs to clarify the role played by the fabrication technique, and in particular the issue of annealing [70]. Review papers by Salluzzo [71] and by Sulpizio *et al.*[72] discuss various experimental aspects related to this point. Note that there are also proposals advocating the existence of two regimes with distinct intrinsic magnetic groundstates separated by a Kondo (spin screened) phase : for low doping (gate voltage) ferromagnetism (see also Ref. [43]) is tied to d_{xy} orbitals while, for optimal doping and beyond, magnetism also involves d_{xz} and d_{yz} states [64, 73].

From a theory perspective, various scenarios designed to explain the occurrence of magnetism have been constructed, some based on intrinsic properties of the 2DEL electronic states and others invoking the role of oxygen vacancies. In the former category a magnetic polarization is mediated at the interface through the coupling with mobile, subsurface electrons. As mentioned above, carriers spatially localized at the interface have d_{xy} symmetry and disorder and/or correlations tend to localize their wavefunctions. Deeper in, on the STO side, one finds states with d_{xy}, d_{xz} and d_{yz} symmetry. RKKY interactions trigger ferromagnetism at the interface if the mobile carriers that are coupled to the interface states are of d_{xy} type [60]. Alternatively, Hund's rule promotes the magnetic instability either through the Zener, P.W Anderson and P.G. de Gennes exchange mechanism (leading to a spiral spin state) [74] or through the enhanced spin polarization of quasi-1D electrons [75] if d_{xz} and d_{yz} orbitals are at play. In the latter category, electrons donated by oxygen vacancies near the interface partly contribute to the conduction band and partly to forming localized states orbiting neighboring Ti sites. Correlations are required to produce a magnetic instability [76, 30, 77] (see also Ref. [70]).

An understanding of the interplay between superconductivity and mag-

netism probably requires one to involve all three t_{2g} orbitals. The magnetic energy scale appears to be so large that it would preclude Cooper pairing if only d_{xy} states were at play. By contrast, estimates of the characteristic magnetic energies pertaining to the d_{xz} and d_{yz} orbitals, giving 1 meV, might not be as adverse to the establishment of superconductivity albeit with a finite momentum for the condensate [60]. Note that orbital selectiveness has been invoked to explain magnetic and superconducting properties of selected oxide families such as the Ruthenates. To conclude this discussion, it is clear that one needs to design specific experimental tests of these theories and in particular of scenarios linking magnetism and superconductivity.

4. The $LaTiO_3/SrTiO_3$ system (LTO/STO)

The interface between the Mott insulator $LaTiO_3$ and $SrTiO_3$ was also found to be superconducting with a value of T_c very close to that of the LAO/STO system. This interesting system presents many similarities with the LAO/STO compound. A detailed account of experiments performed on this heterostructure, mostly in Jérôme Lesueur's group in Paris, can be found in references [78, 79].

5. High T_c heterostructures

Extensive studies of bilayer structures made of underdoped (insulating-I) and overdoped (metallic-M and non-superconducting) $(La_{1-x}Sr_x)CuO_4$ have been performed by the group of Ivan Bozovic in Brookhaven and also in Bremen [80, 81].

It is found that that these bilayers are superconducting with a T_c of 15 K (I-M sequence) or 30 K (M-I sequence). Charge transfer between the different unit cells allows superconductivity to be explained [82]. Exposed to an ozone atmosphere, T_c is boosted to 50 K, a value that is not reached in single-phase films. Possible explanations for this enhancement of T_c include a reduced disorder or the absence of a competing phase in these low-dimensional bilayers. In

another set of experiments, Zn delta-doping was used to selectively suppress T_c in a specific unit cell of the heterostructure. For the M-I structures it was found that T_c is insensitive to the Zn doping in any unit cell of the M-I structures used but in the second one away from the interface, on the I-side. These results suggest that high T_c superconductivity develops in a single CuO_2 plane [7].

6. Surface-induced superconductivity

In recent years, the electrical double layer transistor (EDLT) concept has been applied to oxide compounds (see for instance [83],[9]). This technique allows huge carrier densities of up to a few $10^{15}\,\mathrm{cm}^{-2}$ to be induced even at the surface of insulating compounds. Using insulating STO crystals and the EDLT technique, the groups of Iwasa and Kawasaki successfully demonstrated that superconductivity can be achieved in an insulator through application of an electric field [9]. Soon after this discovery, the same approach was used with ZrNCl [84] allowing large changes in the superconducting transition temperatures to be achieved. Further work allowed superconductivity in the incipient ferroelectric $KTaO_3$ to be induced [10]. This amazing technique allowing very large changes in sheet carrier densities at surfaces creates a pathway for field-gating developments in many other insulating compounds. Also the possibility to use the EDLT technique to chemically modify the materials by applying large gate voltages offers a promising road to tune interface superconductivity.

7. Superconductivity in atomically thin FeSe layers

Evidences for interface superconductivity have also been recently reported in monolayers of FeSe deposited on $SrTiO_3$ substrates [8]. Wang and coworkers observed that when a monolayer of FeSe is deposited on an $SrTiO_3$ substrate by molecular beam epitaxy unexpected superconducting properties are found. While T_c $\sim$9 K[85] for bulk FeSe, tunneling spectra at 4.2 K reveal a superconducting gap Δ $\sim$20 meV in the case of the FeSe/STO heterostructure, one order of magnitude larger than that of the bulk ($\Delta \sim 2.2$ meV [86]). When the

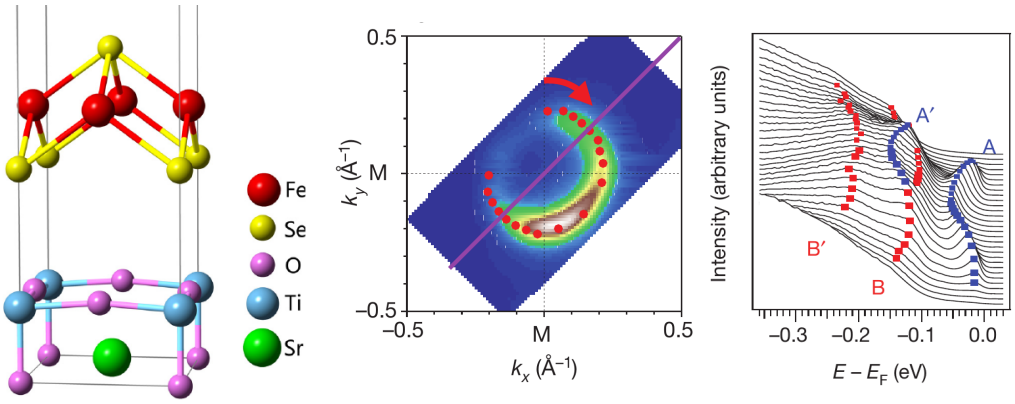

Figure 8: (Left) Atomic structure of a FeSe monolayer deposited on a TiO_2-terminated (001)-oriented $SrTiO_3$ substrate. (From Ref. [89]) (Center) Momentum dependence of the superconducting gap of a single-layer FeSe measured by ARPES at 16 K. (From Ref. [90]) (Right) Energy distribution curves at the M point: the electron-like band (A), crossing the Fermi level, is replicated 100 meV lower in energy (A'). Similarly, the hole-like band (B), located 80 meV below E_F, is also replicated (B'). (From Ref. [90])

thickness of the FeSe film is increased, the value of T_c decreases [87]; similarly, it appears that the effect of a capping layer, added to protect these air sensitive films, is to lower T_c, hampering *ex-situ* characterization. Measurements of the diamagnetic response of one unit cell thick FeSe films by a two-coil mutual inductance technique have recently confirmed the establishment of a superconducting state at ∼21 K, well above the bulk critical temperature [88].

A wealth of information on the electronic properties of the system has come from ARPES measurements. Here the role of possible photo-carriers created by the synchrotron radiation that diffuse to the interface is a topic of consideration. It has been shown that the electronic structure is made of a single band crossing the Fermi level: the Fermi surface consists of electron-like circular pockets centered at the zone edge [91]. Superconductivity appears after an annealing process of the interface at relatively low temperature in vacuum. During this step, the FeSe carrier concentration, as measured by the size of the Fermi surface, is modified. The observed changes could be due to Se evaporation, that would electron dope $FeSe_{1-x}$, or to the creation of oxygen vacancies in $SrTiO_3$, that would also n-dope the system via a transfer to the interface FeSe layer

[92]. Changing the doping by successive annealing steps results in a modulation of the amplitude of the superconducting gap as well as in the value of T_c; low temperature ARPES spectra show a maximum Δ $\sim$20 meV for a T_c of 65 K. The symmetry of the gap in momentum space is circular, pointing to a s-wave superconducting state [91].

Scanning tunneling experiments and ARPES data indicate that only the first atomic layer is superconducting, i.e that the subsequent layers display a semiconducting behavior [8, 93]. Similarly, the Fermi surface topology of the second and third layer changes dramatically [87]. These findings point to a very important role played by the FeSe/STO interface on the observed superconductivity.

A possible mechanism for the increase of T_c could be related to the epitaxial strain [94] experienced by the FeSe layer. For bulk FeSe, raising the external pressure causes a dramatic increase in T_c with a maximum value observed of $\sim$37 K, four times the bulk critical temperature [95]. To investigate this idea, FeSe monolayers have been grown on different oxide substrates; T_c (as estimated from the closing of the gap by ARPES) goes up from 65 K on STO (strain 3.6%)[92, 87] to 70 K on $KTaO_3$ (strain 4.5%) to 75 K on $BaTiO_3$ (strain 5.8%)[96]. The observed dependence on strain is however larger than that one can estimate from the bulk dependence of T_c on pressure.

An appealing scenario to explain this interface superconductivity has been proposed by Lee *et al.* [90]. Measuring high-resolution ARPES spectra, they observed that the electronic bands of the FeSe monolayer are replicated with an energy shift of 100 meV. They attribute this effect to a strong electron-phonon coupling between the layer and the substrate [89]: a phonon mode, most probably an oxygen optical phonon, in $SrTiO_3$ couples to the FeSe electrons. Calculations show that such an interfacial coupling can lead to the increase of the critical temperature observed in the system. This study also confirms that the behavior of a single unit cell thick layer is completely different from a 2 unit cell (or more) thick sample. For thicker films, both electron-like and hole-like bands cross the Fermi level and no superconductivity gap (as well as no replica)

is observed.

Finally, there have been several proposals suggesting that high-T_c superconductivity could be achieved in bilayers of metallic 2D electron systems and highly polarizable materials such as STO, as a result of interface induced pairing. The intensity of the attractive interaction is claimed to be enhanced thanks to a spatial dichotomy between the (super-)conducting layer and the neighboring part of the material where virtual excitations mediate strong pairing [16, 17].

8. Conclusions

In this article, we have discussed several interfacial superconducting systems, placing a particular emphasis on the $LaAlO_3/SrTiO_3$ case. We have highlighted several properties of the $LaAlO_3/SrTiO_3$ heterostructure that appear to be specific consequences of the interface geometry. This is seen when we compare this system with bulk doped $SrTiO_3$. The interfacial nature of the system and the confinement of the electron liquid are key factors that determine the electronic structure of the interface. The breaking of inversion symmetry also leads to a Rashba spin-orbit effect that is tunable with an electric field and that pushes the value of the parallel critical field for the destruction of superconductivity far beyond the Pauli limit. Our brief account of interface superconductivity in transition metal oxides has underscored the broad range of approaches that promote electron pairing. These were discussed in the case of cuprate heterostructures, at crystal surfaces where conductivity and superconductivity can be induced using the electrical double layer transistor field effect technique, or in one monolayer of FeSe deposited on $SrTiO_3$. This field of research will definitely expand at a fast pace in the coming years and promises to hold more great surprises for us.

9. Acknowledgements

This work was supported by the Swiss National Science Foundation, by the Institut Universitaire de France and has received funding from the European Research Council under the European Union Seventh Framework Programme (FP7/2007-2013) / ERC Grant Agreement n.319286 (Q-MAC).

10. References

[1] J. Hirsch, D. Scalapino, Enhanced Superconductivity in Quasi Two-Dimensional Systems, Phys. Rev. Lett. 56 (1986) 2732–2735. doi:10.1103/PhysRevLett.56.2732.

[2] D. Jérome, Superconductivity in New Materials, Elsevier, 2011, Ch. Organic Superconductivity: A Mouse may be of Service to a Lion, p. 149.

[3] A. Ohtomo, H. Y. Hwang, A high-mobility electron gas at the $LaAlO_3/SrTiO_3$ heterointerface., Nature 427 (2004) 423–6. doi:10.1038/nature02308.

[4] N. Reyren, S. Thiel, A. D. Caviglia, L. F. Kourkoutis, G. Hammerl, C. Richter, C. W. Schneider, T. Kopp, A.-S. Rüetschi, D. Jaccard, M. Gabay, D. A. Muller, J.-M. Triscone, J. Mannhart, Superconducting interfaces between insulating oxides., Science 317 (2007) 1196–9. doi:10.1126/science.1146006.

[5] A. D. Caviglia, M. Gabay, S. Gariglio, N. Reyren, C. Cancellieri, J.-M. Triscone, Tunable Rashba Spin-Orbit Interaction at Oxide Interfaces, Phys. Rev. Lett. 104 (2010) 126803. doi:10.1103/PhysRevLett.104.126803.

[6] M. Ben Shalom, M. Sachs, D. Rakhmilevitch, A. Palevski, Y. Dagan, Tuning Spin-Orbit Coupling and Superconductivity at the $SrTiO_3/LaAlO_3$ Interface: A Magnetotransport Study, Phys. Rev. Lett. 104 (2010) 126802. doi:10.1103/PhysRevLett.104.126802.

[7] G. Logvenov, A. Gozar, I. Bozovic, High-Temperature Superconductivity in a Single Copper-Oxygen Plane, Science 326 (2009) 699–702. doi:10.1126/science.1178863.

[8] Q.-Y. Wang, Z. Li, W.-H. Zhang, Z.-C. Zhang, J.-S. Zhang, W. Li, H. Ding, Y.-B. Ou, P. Deng, K. Chang, J. Wen, C.-L. Song, K. He, J.-F. Jia, S.-H. Ji, Y.-Y. Wang, L.-L. Wang, X. Chen, X.-C. Ma, Q.-K. Xue, Interface-Induced

High-Temperature Superconductivity in Single Unit-Cell FeSe Films on $SrTiO_3$, Chin. Phys. Lett. 29 (2012) 037402. doi:10.1088/0256-307X/29/3/037402.

[9] K. Ueno, S. Nakamura, H. Shimotani, A. Ohtomo, N. Kimura, T. Nojima, H. Aoki, Y. Iwasa, M. Kawasaki, Electric-field-induced superconductivity in an insulator, Nat. Mater. 7 (2008) 855–8. doi:10.1038/nmat2298.

[10] K. Ueno, S. Nakamura, H. Shimotani, H. T. Yuan, N. Kimura, T. Nojima, H. Aoki, Y. Iwasa, M. Kawasaki, Discovery of superconductivity in $KTaO_3$ by electrostatic carrier doping, Nat. Nanotechnol. 6 (2011) 408–12. doi:10.1038/nnano.2011.78.

[11] V. L. Ginzburg, On surface superconductivity, Phys. Lett. 13 (1964) 101. doi:10.1016/0031-9163(64)90672-9.

[12] N. S. Sidorov, A. Palnichenko, O. M. Vyaselev, Superconductivity in Mg/MgO interface, Physica C 480 (2012) 123–125. doi:10.1016/j.physc.2012.05.003.

[13] S. Okamoto, T. Maier, Enhanced superconductivity in superlattices of high-T_c cuprates, Phys. Rev. Lett. 101 (2008) 156401. doi:10.1103/PhysRevLett.101.156401.

[14] D. Allender, J. Bray, J. Bardeen, Model for an exciton mechanism of superconductivity, Phys. Rev. B 7 (1973) 1020–1029. doi:10.1103/PhysRevB.7.1020.

[15] W. Little, H. Gutfreund, Dynamic effective electron-electron interaction in the vicinity of a polarizable molecule, Phys. Rev. B 4 (1971) 817–823. doi:10.1103/PhysRevB.4.817.

[16] V. Koerting, Q. Yuan, P. Hirschfeld, T. Kopp, J. Mannhart, Interface-mediated pairing in field effect devices, Phys. Rev. B 71 (2005) 104510. doi:10.1103/PhysRevB.71.104510.

[17] C. Stephanos, T. Kopp, J. Mannhart, P. J. Hirschfeld, Interface-induced d-wave pairing, Phys. Rev. B 84 (2011) 100510. doi:10.1103/PhysRevB.84.100510.

[18] S. N. Klimin, J. Tempere, J. T. Devreese, D. van der Marel, Interface superconductivity in $LaAlO_3$-$SrTiO_3$ heterostructures, Phys. Rev. B 89 (2014) 184514. doi:10.1103/PhysRevB.89.184514.

[19] L. L. Chang, B. C. Giessen (Eds.), Synthetic Modulated Structures, Academic Press, 1985.

[20] J. Mannhart, D. G. Schlom, Oxide interfaces–an opportunity for electronics., Science 327 (2010) 1607–11. doi:10.1126/science.1181862.

[21] P. Zubko, S. Gariglio, M. Gabay, P. Ghosez, J.-M. Triscone, Interface Physics in Complex Oxide Heterostructures, Annu. Rev. Condens. Matter Phys. 2 (2011) 141. doi:10.1146/annurev-conmatphys-062910-140445.

[22] H. Y. Hwang, Y. Iwasa, M. Kawasaki, B. Keimer, N. Nagaosa, Y. Tokura, Emergent phenomena at oxide interfaces, Nat. Mater. 11 (2012) 103–113. doi:10.1038/nmat3223.

[23] A. Ohtomo, D. A. Muller, J. L. Grazul, H. Y. Hwang, Artificial charge-modulation in atomic-scale perovskite titanate superlattices, Nature 419 (2002) 378–380. doi:10.1038/nature00977.

[24] S. Thiel, G. Hammerl, A. Schmehl, C. W. Schneider, J. Mannhart, Tunable quasi-two-dimensional electron gases in oxide heterostructures., Science 313 (2006) 1942–5. doi:10.1126/science.1131091.

[25] N. Nakagawa, H. Y. Hwang, D. A. Muller, Why some interfaces cannot be sharp, Nat. Mater. 5 (2006) 204–209. doi:10.1038/nmat1569.

[26] J. Goniakowski, F. Finocchi, C. Noguera, Polarity of oxide surfaces and nanostructures, Rep. Prog. Phys. 71 (2008) 016501. doi:10.1088/0034-4885/71/1/016501.

[27] R. Pentcheva, W. Pickett, Avoiding the Polarization Catastrophe in $LaAlO_3$ Overlayers on $SrTiO_3$(001) through Polar Distortion, Phys. Rev. Lett. 102 (2009) 107602. doi:10.1103/PhysRevLett.102.107602.

[28] C. Cancellieri, D. Fontaine, S. Gariglio, N. Reyren, A. Caviglia, A. Fête, S. Leake, S. Pauli, P. Willmott, M. Stengel, P. Ghosez, J.-M. Triscone, Electrostriction at the $LaAlO_3/SrTiO_3$ Interface, Phys. Rev. Lett. 107 (2011) 056102. doi:10.1103/PhysRevLett.107.056102.

[29] N. Bristowe, P. Littlewood, E. Artacho, Surface defects and conduction in polar oxide heterostructures, Phys. Rev. B 83 (2011) 205405. doi:10.1103/PhysRevB.83.205405.

[30] L. Yu, A. Zunger, A polarity-induced defect mechanism for conductivity and magnetism at polarnonpolar oxide interfaces, Nat. Commun. 5. doi:10.1038/ncomms6118.

[31] P. Willmott, S. Pauli, R. Herger, C. Schlepütz, D. Martoccia, B. Patterson, B. Delley, R. Clarke, D. Kumah, C. Cionca, Y. Yacoby, Structural Basis for the Conducting Interface between $LaAlO_3$ and $SrTiO_3$, Phys. Rev. Lett. 99 (2007) 155502. doi:10.1103/PhysRevLett.99.155502.

[32] A. S. Kalabukhov, Y. A. Boikov, I. T. Serenkov, V. I. Sakharov, V. N. Popok, R. Gunnarsson, J. Borjesson, N. Ljustina, E. Olsson, D. Winkler, T. Claeson, Cationic Disorder and Phase Segregation in $LaAlO_3/SrTiO_3$ Heterointerfaces Evidenced by Medium-Energy Ion Spectroscopy, Phys. Rev. Lett. 103 (2009) 146101. doi:10.1103/PhysRevLett.103.146101.

[33] N. C. Bristowe, P. Ghosez, P. B. Littlewood, E. Artacho, The origin of two-dimensional electron gases at oxide interfaces: insights from theory., J. Phys. Condens. Matter 26 (2014) 143201. doi:10.1088/0953-8984/26/14/143201.

[34] O. Copie, V. Garcia, C. Bodefeld, C. Carretero, M. Bibes, G. Herranz, E. Jacquet, J.-L. Maurice, B. Vinter, S. Fusil, K. Bouzehouane,

H. Jaffres, A. Barthelemy, Towards Two-Dimensional Metallic Behavior at $LaAlO_3/SrTiO_3$ Interfaces, Phys. Rev. Lett. 102 (2009) 216804. doi:10.1103/PhysRevLett.102.216804.

[35] A. Dubroka, M. Rössle, K. W. Kim, V. K. Malik, L. Schultz, S. Thiel, C. W. Schneider, J. Mannhart, G. Herranz, O. Copie, M. Bibes, A. Barthélémy, C. Bernhard, Dynamical Response and Confinement of the Electrons at the $LaAlO_3/SrTiO_3$ Interface, Phys. Rev. Lett. 104 (2010) 156807. doi:10.1103/PhysRevLett.104.156807.

[36] N. Reyren, S. Gariglio, A. D. Caviglia, D. Jaccard, T. Schneider, J.-M. Triscone, Anisotropy of the superconducting transport properties of the $LaAlO_3/SrTiO_3$ interface, Appl. Phys. Lett. 94 (2009) 112506. doi:10.1063/1.3100777.

[37] P. Delugas, A. Filippetti, V. Fiorentini, D. I. Bilc, D. Fontaine, P. Ghosez, Spontaneous 2-Dimensional Carrier Confinement at the n-Type $SrTiO_3/LaAlO_3$ Interface, Phys. Rev. Lett. 106 (2011) 166807. doi:10.1103/PhysRevLett.106.166807.

[38] W. Son, E. Cho, B. Lee, J. Lee, S. Han, Density and spatial distribution of charge carriers in the intrinsic n-type $LaAlO_3$-$SrTiO_3$ interface, Phys. Rev. B 79 (2009) 245411. doi:10.1103/PhysRevB.79.245411.

[39] M. Salluzzo, J. C. Cezar, N. B. Brookes, V. Bisogni, G. M. De Luca, C. Richter, S. Thiel, J. Mannhart, M. Huijben, A. Brinkman, G. Rijnders, G. Ghiringhelli, Orbital Reconstruction and the Two-Dimensional Electron Gas at the $LaAlO_3/SrTiO_3$ Interface, Phys. Rev. Lett. 102 (2009) 166804. doi:10.1103/PhysRevLett.102.166804.

[40] M. Breitschaft, V. Tinkl, N. Pavlenko, S. Paetel, C. Richter, J. R. Kirtley, Y. C. Liao, G. Hammerl, V. Eyert, T. Kopp, J. Mannhart, Two-dimensional electron liquid state at $LaAlO_3$-$SrTiO_3$ interfaces, Phys. Rev. B 81 (2010) 153414. doi:10.1103/PhysRevB.81.153414.

[41] W. Meevasana, X. J. Zhou, B. Moritz, C.-C. Chen, R. H. He, S.-I. Fujimori, D. H. Lu, S.-K. Mo, R. G. Moore, F. Baumberger, T. P. Devereaux, D. van der Marel, N. Nagaosa, J. Zaanen, Z.-X. Shen, Strong energy-momentum dispersion of phonon-dressed carriers in the lightly doped band insulator $SrTiO_3$, New J. Phys. 12 (2010) 23004. doi:10.1088/1367-2630/12/2/023004.

[42] C. Richter, H. Boschker, W. Dietsche, E. Fillis-Tsirakis, R. Jany, F. Loder, L. F. Kourkoutis, D. a. Muller, J. R. Kirtley, C. W. Schneider, J. Mannhart, Interface superconductor with gap behaviour like a high-temperature superconductor, Nature 502 (2013) 528–31. doi:10.1038/nature12494.

[43] A. Brinkman, M. Huijben, M. van Zalk, J. Huijben, U. Zeitler, J. C. Maan, W. G. van der Wiel, G. Rijnders, D. H. A. Blank, H. Hilgenkamp, Magnetic effects at the interface between non-magnetic oxides, Nat. Mater. 6 (2007) 493–496. doi:10.1038/nmat1931.

[44] L. Li, C. Richter, J. Mannhart, R. C. Ashoori, Coexistence of magnetic order and two-dimensional superconductivity at $LaAlO_3/SrTiO_3$ interfaces, Nat. Phys. 7 (2011) 762–766. doi:10.1038/nphys2080.

[45] J. A. Bert, B. Kalisky, C. Bell, M. Kim, Y. Hikita, H. Y. Hwang, K. A. Moler, Direct imaging of the coexistence of ferromagnetism and superconductivity at the $LaAlO_3/SrTiO_3$ interface, Nat. Phys. 7 (2011) 767–771. doi:10.1038/nphys2079.

[46] D. A. Dikin, M. Mehta, C. W. Bark, C. M. Folkman, C. B. Eom, V. Chandrasekhar, Coexistence of Superconductivity and Ferromagnetism in Two Dimensions, Phys. Rev. Lett. 107 (2011) 056802. doi:10.1103/PhysRevLett.107.056802.

[47] L. Benfatto, C. Castellani, T. Giamarchi, Broadening of the Berezinskii-Kosterlitz-Thouless superconducting transition by inhomogeneity and finite-size effects, Phys. Rev. B 80 (2009) 214506. doi:10.1103/PhysRevB.80.214506.

[48] S. Caprara, M. Grilli, L. Benfatto, C. Castellani, Effective medium theory for superconducting layers: A systematic analysis including space correlation effects, Phys. Rev. B 84 (2011) 014514. doi:10.1103/PhysRevB.84.014514.

[49] S. Caprara, F. Peronaci, M. Grilli, Intrinsic Instability of Electronic Interfaces with Strong Rashba Coupling, Phys. Rev. Lett. 109 (2012) 196401. doi:10.1103/PhysRevLett.109.196401.

[50] S. Caprara, J. Biscaras, N. Bergeal, D. Bucheli, S. Hurand, C. Feuillet-Palma, A. Rastogi, R. Budhani, J. Lesueur, M. Grilli, Multiband superconductivity and nanoscale inhomogeneity at oxide interfaces, Phys. Rev. B 88 (2013) 020504. doi:10.1103/PhysRevB.88.020504.

[51] B. Spivak, P. Oreto, S. Kivelson, Theory of quantum metal to superconductor transitions in highly conducting systems, Phys. Rev. B 77 (2008) 214523. doi:10.1103/PhysRevB.77.214523.

[52] J. Schooley, W. R. Hosler, M. L. Cohen, Superconductivity In Semiconducting $SrTiO_3$, Phys. Rev. Lett. 12 (1964) 474. doi:10.1103/PhysRevLett.12.474.

[53] J. Schooley, W. Hosler, E. Ambler, J. Becker, M. Cohen, C. Koonce, Dependence of the Superconducting Transition Temperature on Carrier Concentration in Semiconducting $SrTiO_3$, Phys. Rev. Lett. 14 (1965) 305–307. doi:10.1103/PhysRevLett.14.305.

[54] C. S. Koonce, M. L. Cohen, J. Schooley, W. R. Hosler, E. R. Pfeiffer, Superconducting Transition Temperatures Of Semiconducting $SrTiO_3$, Phys. Rev. 163 (1967) 380. doi:10.1103/PhysRev.163.380.

[55] X. Lin, G. Bridoux, A. Gourgout, G. Seyfarth, S. Krämer, M. Nardone, B. Fauqué, K. Behnia, Critical Doping for the Onset of a Two-Band Superconducting Ground State in $SrTiO_{3-\delta}$, Phys. Rev. Lett. 112 (2014) 207002. doi:10.1103/PhysRevLett.112.207002.

[56] A. Fête, S. Gariglio, A. Caviglia, J.-M. Triscone, M. Gabay, Rashba induced magnetoconductance oscillations in the $LaAlO_3$-$SrTiO_3$ heterostructure, Phys. Rev. B 86 (2012) 201105. doi:10.1103/PhysRevB.86.201105.

[57] J. Bert, K. Nowack, B. Kalisky, H. Noad, J. Kirtley, C. Bell, H. Sato, M. Hosoda, Y. Hikita, H. Hwang, K. Moler, Gate-tuned superfluid density at the superconducting $LaAlO_3/SrTiO_3$ interface, Phys. Rev. B 86 (2012) 060503. doi:10.1103/PhysRevB.86.060503.

[58] J. R. Kirtley, B. Kalisky, J. a. Bert, C. Bell, M. Kim, Y. Hikita, H. Y. Hwang, J. H. Ngai, Y. Segal, F. J. Walker, C. H. Ahn, K. a. Moler, Scanning SQUID susceptometry of a paramagnetic superconductor, Phys. Rev. B 85 (2012) 224518. doi:10.1103/PhysRevB.85.224518.

[59] O. Dimitrova, M. Feigelman, Theory of a two-dimensional superconductor with broken inversion symmetry, Phys. Rev. B 76 (2007) 014522. doi:10.1103/PhysRevB.76.014522.

[60] K. Michaeli, A. C. Potter, P. A. Lee, Superconducting and Ferromagnetic Phases in $SrTiO_3/LaAlO_3$ Oxide Interface Structures: Possibility of Finite Momentum Pairing, Phys. Rev. Lett. 108 (2012) 117003. doi:10.1103/PhysRevLett.108.117003.

[61] F. Loder, A. P. Kampf, T. Kopp, Superconductivity with Rashba spin-orbit coupling and magnetic field., J. Phys. Condens. Matter 25 (2013) 362201. doi:10.1088/0953-8984/25/36/362201.

[62] Y. Nakamura, Y. Yanase, Multi-Orbital Fulde-Ferrell-Larkin-Ovchinnikov State in $SrTiO_3$ Heterostructures, con-mat.supr.con arXiv:1408.4927.

[63] J.-S. Lee, Y. W. Xie, H. K. Sato, C. Bell, Y. Hikita, H. Y. Hwang, C.-C. Kao, Titanium d_{xy} ferromagnetism at the $LaAlO_3/SrTiO_3$interface, Nat. Mater. 12 (2013) 703–6. doi:10.1038/nmat3674.

[64] F. Bi, M. Huang, S. Ryu, H. Lee, C.-W. Bark, C.-B. Eom, P. Irvin, J. Levy, Room-temperature electronically-controlled ferromagnetism at the

$LaAlO_3/SrTiO_3$ interface, Nat. Commun. 5 (2014) 5019. doi:10.1038/ncomms6019.

[65] B. Kalisky, J. A. Bert, B. B. Klopfer, C. Bell, H. K. Sato, M. Hosoda, Y. Hikita, H. Y. Hwang, K. A. Moler, Critical thickness for ferromagnetism in $LaAlO_3/SrTiO_3$ heterostructures., Nat. Commun. 3 (2012) 922. doi:10.1038/ncomms1931.

[66] A. F. Santander-Syro, F. Fortuna, C. Bareille, T. C. Rödel, G. Landolt, N. C. Plumb, J. H. Dil, M. Radović, Giant spin splitting of the two-dimensional electron gas at the surface of $SrTiO_3$., Nat. Mater. 13 (2014) 1085–1090. doi:10.1038/nmat4107.

[67] G. Berner, M. Sing, H. Fujiwara, A. Yasui, Y. Saitoh, A. Yamasaki, Y. Nishitani, A. Sekiyama, N. Pavlenko, T. Kopp, C. Richter, J. Mannhart, S. Suga, R. Claessen, Direct k-Space Mapping of the Electronic Structure in an Oxide-Oxide Interface, Phys. Rev. Lett. 110 (2013) 247601. doi:10.1103/PhysRevLett.110.247601.

[68] M. Fitzsimmons, N. Hengartner, S. Singh, M. Zhernenkov, F. Bruno, J. Santamaria, A. Brinkman, M. Huijben, H. Molegraaf, J. de la Venta, I. Schuller, Upper Limit to Magnetism in $LaAlO_3/SrTiO_3$ Heterostructures, Phys. Rev. Lett. 107 (2011) 217201. doi:10.1103/PhysRevLett.107.217201.

[69] Z. Salman, O. Ofer, M. Radovic, H. Hao, M. Ben Shalom, K. H. Chow, Y. Dagan, M. D. Hossain, C. D. P. Levy, W. A. MacFarlane, G. M. Morris, L. Patthey, M. R. Pearson, H. Saadaoui, T. Schmitt, D. Wang, R. F. Kiefl, Nature of Weak Magnetism in $SrTiO_3/LaAlO_3$ Multilayers, Phys. Rev. Lett. 109 (2012) 257207. doi:10.1103/PhysRevLett.109.257207.

[70] M. Salluzzo, S. Gariglio, D. Stornaiuolo, V. Sessi, S. Rusponi, C. Piamonteze, G. M. De Luca, M. Minola, D. Marré, A. Gadaleta, H. Brune, F. Nolting, N. B. Brookes, G. Ghiringhelli, Origin of Interface Magnetism in

$BiMnO_3/SrTiO_3$ and $LaAlO_3/SrTiO_3$ Heterostructures, Phys. Rev. Lett. 111 (2013) 087204. doi:10.1103/PhysRevLett.111.087204.

[71] M. Salluzzo, Oxide Thin Films, Multilayers and Nanocomposites, Springer International Publishing AG, 2015, Ch. Electronic reconstruction at the interface between band insulating oxides: the $LaAlO_3/SrTiO_3$ system.

[72] J. A. Sulpizio, S. Ilani, P. Irvin, J. Levy, Nanoscale Phenomena in Oxide Heterostructures, Annu. Rev. Mater. Res. 44 (2014) 117–149. doi:10.1146/annurev-matsci-070813-113437.

[73] J. Ruhman, A. Joshua, S. Ilani, E. Altman, Competition between Kondo screening and magnetism at the $LaAlO_3/SrTiO_3$ interface, Phys. Rev. B 90 (2014) 125123. doi:10.1103/PhysRevB.90.125123.

[74] S. Banerjee, O. Erten, M. Randeria, Ferromagnetic exchange, spin-orbit coupling and spiral magnetism at the $LaAlO_3/SrTiO_3$ interface, Nat. Phys. 9 (2013) 626–630. doi:10.1038/nphys2702.

[75] G. Chen, L. Balents, Ferromagnetism in Itinerant Two-Dimensional t_{2g} Systems, Phys. Rev. Lett. 110 (2013) 206401. doi:10.1103/PhysRevLett.110.206401.

[76] N. Pavlenko, T. Kopp, E. Tsymbal, G. Sawatzky, J. Mannhart, Magnetic and superconducting phases at the $LaAlO_3/SrTiO_3$ interface: The role of interfacial Ti $3d$ electrons, Phys. Rev. B 85 (2012) 020407. doi:10.1103/PhysRevB.85.020407.

[77] F. Lechermann, L. Boehnke, D. Grieger, C. Piefke, Electron correlation and magnetism at the $LaAlO_3/SrTiO_3$ interface: A DFT+DMFT investigation, Phys. Rev. B 90 (2014) 085125. doi:10.1103/PhysRevB.90.085125.

[78] J. Biscaras, N. Bergeal, A. Kushwaha, T. Wolf, A. Rastogi, R. C. Budhani, J. Lesueur, Two-dimensional superconductivity at a Mott insulator/band insulator interface $LaTiO_3/SrTiO_3$, Nat. Commun. 1 (2010) 89. doi:10.1038/ncomms1084.

[79] J. Biscaras, N. Bergeal, S. Hurand, C. Feuillet-Palma, A. Rastogi, R. C. Budhani, M. Grilli, S. Caprara, J. Lesueur, Multiple quantum criticality in a two-dimensional superconductor., Nat. Mater. 12 (2013) 542–8. doi:10.1038/nmat3624.

[80] A. Gozar, G. Logvenov, L. F. Kourkoutis, A. T. Bollinger, L. A. Giannuzzi, D. A. Muller, I. Bozovic, High-temperature interface superconductivity between metallic and insulating copper oxides, Nature 455 (2008) 782–785. doi:http://dx.doi.org/10.1038/nature07293.

[81] J. Pereiro, A. Petrovic, C. Panagopoulos, I. Božović, Interface superconductivity: History, development and prospects, Phys. Express 1 (2011) 208.

[82] S. Smadici, J. Lee, S. Wang, P. Abbamonte, G. Logvenov, A. Gozar, C. Cavellin, I. Bozovic, Superconducting Transition at 38 K in Insulating-Overdoped La_2CuO_4-$La_{1.64}Sr_{0.36}CuO_4$ Superlattices: Evidence for Interface Electronic Redistribution from Resonant Soft X-Ray Scattering, Phys. Rev. Lett. 102 (2009) 107004. doi:10.1103/PhysRevLett.102.107004.

[83] R. Misra, M. McCarthy, A. F. Hebard, Electric field gating with ionic liquids, Appl. Phys. Lett. 90 (2007) 052905. doi:10.1063/1.2437663.

[84] J. T. Ye, S. Inoue, K. Kobayashi, Y. Kasahara, H. T. Yuan, H. Shimotani, Y. Iwasa, Liquid-gated interface superconductivity on an atomically flat film, Nat. Mater. 9 (2010) 125–8. doi:10.1038/nmat2587.

[85] F.-C. Hsu, J.-Y. Luo, K.-W. Yeh, T.-K. Chen, T.-W. Huang, P. M. Wu, Y.-C. Lee, Y.-L. Huang, Y.-Y. Chu, D.-C. Yan, M.-K. Wu, Superconductivity in the PbO-type structure α-FeSe, Proc. Nat. Acad. Sci. 105 (2008) 14262–14264. doi:10.1073/pnas.0807325105.

[86] C.-L. Song, Y.-L. Wang, P. Cheng, Y.-P. Jiang, W. Li, T. Zhang, Z. Li, K. He, L. Wang, J.-F. Jia, H.-H. Hung, C. Wu, X. Ma, X. Chen, Q.-K. Xue, Direct Observation of Nodes and Twofold Symmetry in FeSe Superconductor, Science 332 (2011) 1410–1413. doi:10.1126/science.1202226.

[87] S. Tan, Y. Zhang, M. Xia, Z. Ye, F. Chen, X. Xie, R. Peng, D. Xu, Q. Fan, H. Xu, J. Jiang, T. Zhang, X. Lai, T. Xiang, J. Hu, B. Xie, D. Feng, Interface-induced superconductivity and strain-dependent spin density waves in FeSe/$SrTiO_3$ thin films, Nat. Mater. 12 (2013) 634–640. doi:10.1038/nmat3654.

[88] W.-H. Zhang, Y. Sun, J.-S. Zhang, F.-S. Li, M.-H. Guo, Y.-F. Zhao, H.-M. Zhang, J.-P. Peng, Y. Xing, H.-C. Wang, T. Fujita, A. Hirata, Z. Li, H. Ding, C.-J. Tang, M. Wang, Q.-Y. Wang, K. He, S.-H. Ji, X. Chen, J.-F. Wang, Z.-C. Xia, L. Li, Y.-Y. Wang, J. Wang, L.-L. Wang, M.-W. Chen, Q.-K. Xue, X.-C. Ma, Direct Observation of High-Temperature Superconductivity in One-Unit-Cell FeSe Films, Chin. Phys. Lett. 31 (2014) 017401. doi:10.1088/0256-307X/31/1/017401.

[89] B. Li, Z. W. Xing, G. Q. Huang, D. Y. Xing, Electron-phonon coupling enhanced by the FeSe/$SrTiO_3$ interface, J. Appl. Phys. 115 (2014) 193907. doi:10.1063/1.4876750.

[90] J. J. Lee, F. T. Schmitt, R. G. Moore, S. Johnston, Y.-T. Cui, W. Li, M. Yi, Z. K. Liu, M. Hashimoto, Y. Zhang, D. H. Lu, T. P. Devereaux, D.-H. Lee, Z.-X. Shen, Interfacial mode coupling as the origin of the enhancement of T_c in FeSe films on $SrTiO_3$, Nature 515 (2014) 245–248. doi:10.1038/nature13894.

[91] D. Liu, W. Zhang, D. Mou, J. He, Y.-B. Ou, Q.-Y. Wang, Z. Li, L. Wang, L. Zhao, S. He, Y. Peng, X. Liu, C. Chen, L. Yu, G. Liu, X. Dong, J. Zhang, C. Chen, Z. Xu, J. Hu, X. Chen, X. Ma, Q. Xue, X. Zhou, Electronic origin of high-temperature superconductivity in single-layer FeSe superconductor, Nat. Commun. 3 (2012) 931. doi:10.1038/ncomms1946.

[92] S. He, J. He, W. Zhang, L. Zhao, D. Liu, X. Liu, D. Mou, Y.-B. Ou, Q.-Y. Wang, Z. Li, L. Wang, Y. Peng, Y. Liu, C. Chen, L. Yu, G. Liu, X. Dong, J. Zhang, C. Chen, Z. Xu, X. Chen, X. Ma, Q. Xue, X. J. Zhou, Phase diagram and electronic indication of high-temperature superconductivity

at 65 K in single-layer FeSe films, Nat. Mater. 12 (2013) 605–610. doi:http://dx.doi.org/10.1038/nmat3648.

[93] X. Liu, D. Liu, W. Zhang, J. He, L. Zhao, S. He, D. Mou, F. Li, C. Tang, Z. Li, L. Wang, Y. Peng, Y. Liu, C. Chen, L. Yu, G. Liu, X. Dong, J. Zhang, C. Chen, Z. Xu, X. Chen, X. Ma, Q. Xue, X. J. Zhou, Dichotomy of the electronic structure and superconductivity between single-layer and double-layer FeSe/$SrTiO_3$ films., Nat. Commun. 5 (2014) 5047. doi:10.1038/ncomms6047.

[94] J. Locquet, J. Perret, J. Fompeyrine, E. Mächler, J. Seo, G. Van Tendeloo, Doubling the critical temperature of $La_{1.9}Sr_{0.1}CuO_4$ using epitaxial strain, Nature 394 (1998) 453–456. doi:10.1038/28810.

[95] S. Medvedev, T. M. McQueen, I. A. Troyan, T. Palasyuk, M. I. Eremets, R. J. Cava, S. Naghavi, F. Casper, V. Ksenofontov, G. Wortmann, C. Felser, Electronic and magnetic phase diagram of β-$Fe_{1.01}Se$ with superconductivity at 36.7 K under pressure, Nat. Mater. 8 (2009) 630–633. doi:http://dx.doi.org/10.1038/nmat2491.

[96] R. Peng, H. C. Xu, S. Y. Tan, H. Y. Cao, M. Xia, X. P. Shen, Z. C. Huang, C. Wen, Q. Song, T. Zhang, B. P. Xie, X. G. Gong, D. L. Feng, Tuning the band structure and superconductivity in single-layer FeSe by interface engineering., Nat. Commun. 5 (2014) 5044. doi:10.1038/ncomms6044.